Generalized Admittance Matrix Method for Fast Full-Wave Analysis of Integrated Lens Antennas

Erik Jørgensen[1], Peter Meincke [1], Andrea Neto[2], Nuria Llombart[2]
[1]TICRA, Copenhagen, Denmark, ej@ticra.com, pme@ticra.com
[2]TU Delft, Delft, The Netherlands, A.Neto@tudelft.nl, N.LlombartJuan@tudelft.nl

***Abstract*—This paper presents an efficient technique for full-wave analysis of dielectric lenses with integrated feeding. The feeding section is analysed with a higher-order 3D-MoM algorithm, while the rotationally symmetric lens is analysed with a higher-order BoR-MoM. Each method allows the extraction of a generalized admittance matrix that fully characterizes the region in question. The individual matrices are finally combined to form the overall admittance matrix, which may subsequently be used to compute all desired quantities (scattering parameters or fields). The method is well-suited for optimization, since a change of the geometry inside an isolated region does not require recomputation of other admittance matrices. The proposed method provides a full-wave solution of typical integrated lens antennas in 1-2 minutes.**

***Index Terms*—Generalized admittance matrix, higher-order MoM, leaky lens, domain decomposition.**

I. Introduction

Dielectric lens antennas with integrated feed/receivers are commonly applied in mm- or sub-mm wave sensing systems. The antenna may be resonant, e.g. [1], or may be designed for UWB operation [2]. In particular, the latter work demonstrated an antenna with constant phase centre and good dispersion properties over a very large bandwidth. Integrated lens antennas are challenging from an EM modeling point of view, since they combine an electrically large lens, including matching layers, with a tightly integrated feed structure. The lens is typically designed using GO or PO approximations which may lead to loss of accuracy in case of resonances or multiple reflections [3]. At the same time, the high-frequency methods do not accurately include the coupling between the feeding structure and the lens. Alternatively, general-purpose full-wave tools can be used but the typical runtime is measured in hours. These methods are therefore not suitable for design optimization, such as shaping of the lens surface.

This paper describes a domain-decomposition method, that allows a full-wave analysis of typical integrated lens antennas in 1-2 minutes. The method includes both the feeding structure and the lens, as well as all coupling effects. The algorithm is based on [4]-[5], that combined four efficient solvers (3D-MoM, BoR-MoM, Mode-matching, and PO) with a generalized admittance matrix framework. This approach allows a scattering or radiation problem to be subdivided into any number of domains, and the admittance matrix of each domain is then obtained using the most suitable solver for the specific domain. The domain boundaries are denoted *radiation ports* and these are located in free space. In this work, we have extended the method to allow the radiation port surface, i.e. the domain boundary, to be placed at the interface between two homogeneous dielectric mediums. This opens up a new range of applications, e.g., analysis of integrated lens antennas. In order to illustrate the capabilities of the proposed method, we apply the method to the planarly fed leaky lens antenna suggested in [2].

II. Generalized Admittance Matrix Approach and Higher-Order MoM

A generalized admittance matrix method for analysis of rotationally symmetric reflector antennas with 3D parts was presented in [4]-[5]. The method is based on a domain decomposition scheme, in which the problem is first subdivided into a number of domains. The domain boundaries are typically located in free space and are denoted radiation ports. The port surfaces are closed by a PEC and an equivalent magnetic port current is defined as $\mathbf{M}^p(\mathbf{r}) = -\hat{n} \times \mathbf{E}(\mathbf{r})$. The magnetic port current is now expanded as

$$\mathbf{M}^p(\mathbf{r}) = \eta_0 \sum_{i=1}^{N^p} V_i \mathbf{M}_i^p, \tag{1}$$

where η_0 is the free space impedance and N^p is the number of port expansion function. In [4], we show that the generalized admittance matrix of a region can be found as

$$[Y] = [Q] \, [Z]^{-1} \, [P] \, . \tag{2}$$

In this equation, $[Z]$ is the standard MoM impedance matrix, and the matrices $[Q]$ and $[P]$ are given by

$$[Q] = \left\langle \mathbf{W}_j^p; -\hat{n} \times \mathbf{J}_t \right\rangle , \tag{3}$$

$$[P] = \left\langle \mathbf{T}_s; \hat{n} \times \mathbf{M}_i^p + \nabla \times \int_{S^p} \mathbf{M}_i^p G \; dS' \right\rangle , \tag{4}$$

in which $\mathbf{W}_j^p$ and $\mathbf{M}_i^p$ are port weighting and expansion functions, respectively, while $\mathbf{T}_s$ and $\mathbf{J}_t$ are MoM weighting and expansion functions, respectively. When the admittance matrix of each region has been evaluated using (2), the overall admittance matrix can be evaluated by eliminating connected port functions through standard cascading operations. This allows the coefficients V_i in (1) to be computed on all

domain boundaries. Finally, the coefficients to the MoM basis functions can be determined from

$$[I] = [Z]^{-1}\,[P]\,[V]\,. \tag{5}$$

The choice of port expansion functions $\mathbf{M}_i^p$, as well as MoM basis and weighting functions, will have a major impact on the efficiency of the method. The port currents are expanded using basis functions with rotational symmetry,

$$\mathbf{M}_i^{p,t,\binom{e}{o}}(t,\phi) = \frac{\mathbf{a}_t}{\mathcal{J}_s(t,\phi)}\widetilde{P}_n(t)\begin{pmatrix}\cos m\phi\\ \sin m\phi\end{pmatrix}, \tag{6a}$$

$$\mathbf{M}_i^{p,\phi,\binom{e}{o}}(t,\phi) = \frac{\mathbf{a}_\phi}{\mathcal{J}_s(t,\phi)}P_n(t)\begin{pmatrix}\cos m\phi\\ \sin m\phi\end{pmatrix}, \tag{6b}$$

where $\mathbf{a}_t = \partial\mathbf{r}/\partial t$, $\mathbf{a}_\phi = \partial\mathbf{r}/\partial\phi$, and $\mathcal{J}_s(t,\phi) = |\mathbf{a}_t \times \mathbf{a}_\phi|$. The azimuthal mode index m is in the range $[0; m^{\max}]$ where $m^{\max}$ must be chosen sufficiently high to ensure an accurate representation of the port currents. The polynomials $P_n(t)$ in (6b) are Legendre polynomials and the polynomials $\widetilde{P}_n(t)$ are the modified Legendre polynomials

$$\widetilde{P}_n(t) = \begin{cases} 1-t, & n=0\\ 1+t, & n=1\\ P_n(t) - P_{n-2}(t), & n\geq 2\end{cases}. \tag{7}$$

The rotationally symmetric port functions imply that a fast BoR-MoM solver can be used to extract admittance matrices of rotationally symmetric regions. The BoR-MoM solver uses basis and weighting functions similar to those in Eq. (6) whereas the 3D-MoM solver uses the higher-order hierarchical Legendre basis functions from [6].

The generalized admittance matrix method described above can be applied to integrated lens problems if the radiation port is placed at the lower face of the lens, separating the 3D feed region from the lens. This implies that the radiation port surface is no longer located in free space but at the boundary between two mediums with different dielectric constants. This requires that the polynomial order and azimuthal expansion order in (6) is adjusted to fit the expected variation of the electric field in the densest medium. Furthermore, the discretization used by the MoM solvers, even in the 3D region where no dielectric material is present, must allow a rapid variation of the electric surface current density on the PEC patches overlapping the radiation port. In this work, we have solved this problem elegantly by exploiting the hierarchical feature of the higher-order Legendre basis functions. The polynomial expansion order used to represent the electric surface current density is automatically increased locally such that the discretization on the port surface, but not anywhere else, matches the fast field variation predicted by $\mathbf{M}^p(\mathbf{r})$.

III. Application Example

The method described above is now applied to the planarly fed leaky lens antenna proposed in [2] which has a wide operating frequency band from 20 GHz to 60 GHz. The lens is composed of a hemisphere of diameter 25 mm and a cylindrical base of height 3.75 mm. The relative permittivity is $\epsilon_r = 10$ and the lens has three matching layers with permittivities of 6.5, 3.5, and 2.5. The lens is fed by an enhanced leaky wave slot (width 0.5 mm) that sits below an air gap (height 250 μm). In this work we employ a simplified feeding of the slot by placing a centre-fed wire below the slot. A schematic drawing of the lens is shown in Figure 1 and the reader is referred to [2] for details.

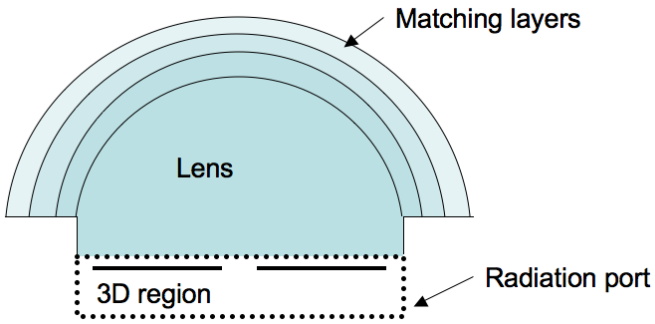

Fig. 1. Schematic drawing illustrating the extended hemispherical lens with three matching layers. The radiation port boundary is shown with a dashed line. A part of the radiation port surface is conformal to the lower face of the lens.

The domain-decomposition method is now applied by introducing a radiation port that separates the 3D feeding section from the rotationally symmetric lens. The radiation port surface is shown with a dashed line in Figure 1. The radiation port is overlapping the lower face of the lens which implies that a part of the radiation port separates two different dielectric materials, whereas the remaining part of the radiation port is located in free space. The admittance matrix of the region inside the radiation port surface is extracted using higher-order 3D-MoM and the admittance matrix of the exterior region is extracted using BoR-MoM. The admittance matrices are then combined by standard cascading techniques which leads to the overall admittance matrix. This allows evaluation of the coefficients to the port expansion functions and the MoM basis functions. The mesh of the antenna is shown in Figure 2. It can be observed that the 3D-MoM solver uses quadrilateral patches with curved edges whereas the BoR-MoM solver uses curved rotationally symmetric patches. This implies that very few patches are needed to model the antenna geometry accurately.

The number of unknowns in the two regions, as well as the number of port expansion functions on the boundary separating the regions, are listed in table I. The number of azimuthal modes is fixed at 16 ($m = 0, .., 15$) which is sufficient for reaching the desired accuracy across the frequency band. This is illustrated in Figure 3 that shows the azimuthal mode power spectrum. The modes with even mode indices are not excited and may be left out. This option is supported by the developed software tool but the number of unknowns and CPU times are reported here with all modes included to illustrate the computation time when no symmetry exists in the 3D region. It should be noted that the relatively low number of unknowns listed in Table I is a consequence of the

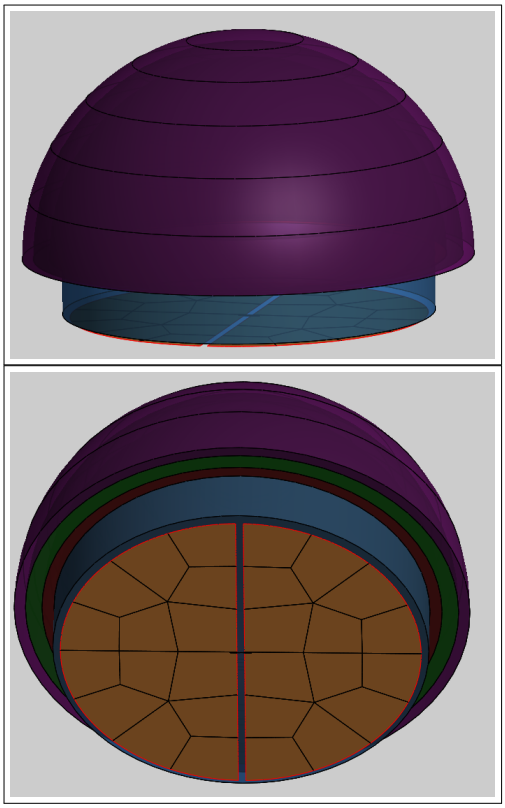

Fig. 2. Meshed model of the planarly fed leaky lens antenna seen from two different angles.

higher-order expansions used for all unknown quantities. The computation time per frequency point is between 13 seconds at the lowest frequency and 126 seconds at the highest. A detailed list of the computation is provided in Table II where it can be observed that the 3D region is the most time-consuming part. Consequently, the time for updating the solution after a change of the lens region is substantially faster which is important when optimising the lens shape. For example, at 20 GHz the full solution can be recomputed in 5 seconds if the 3D region is unchanged. This enables fast optimisation of the lens shape without resorting to asymptotic methods.

TABLE I
NUMBER OF BOR-MOM UNKNOWNS, 3D-MOM UNKNOWNS, AND NUMBER OF PORT FUNCTIONS. THE NUMBER OF AZIMUTHAL MODES IS 16 ($m = 0, .., 15$)

	BoR-MoM	3D-MoM	Port functions	
			Per az. mode	Total
20 GHz	563	3502	44	1364
25 GHz	663	4102	52	1612
30 GHz	735	4538	56	1736
35 GHz	825	5622	74	2294
40 GHz	835	6844	80	2480
45 GHz	911	6940	80	2480
50 GHz	1003	9036	96	2976
55 GHz	1055	9440	108	3348
60 GHz	1223	10966	112	3472

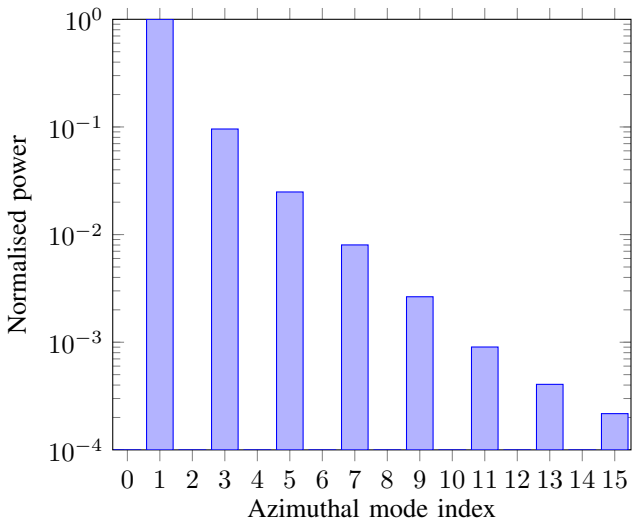

Fig. 3. Power contained in each azimuthal mode normalised to the power of the $m = 1$ mode. The frequency is 60 GHz.

TABLE II
COMPUTATION TIME PER FREQUENCY POINT FOR FULL-WAVE ANALYSIS OF THE PLANARLY FED LEAKY LENS ANTENNA WITH THREE MATCHING LAYERS (2 X XEON E5-2690 @ 2.90GHZ).

	Lens region	3D region	Port elimination	Total
20 GHz	4 s	8 s	1 s	13 s
25 GHz	7 s	10 s	2 s	19 s
30 GHz	10 s	13 s	3 s	26 s
35 GHz	14 s	16 s	7 s	37 s
40 GHz	17 s	22 s	9 s	48 s
45 GHz	22 s	24 s	9 s	55 s
50 GHz	27 s	42 s	15 s	84 s
55 GHz	30 s	48 s	22 s	100 s
60 GHz	35 s	66 s	25 s	126 s

The normalised radiation patterns of the planarly fed leaky lens antenna are shown in Figure 4 for six frequencies between 35 GHz and 60 GHz. The simulated patterns obtained by the generalized admittance matrix method are compared to the measured patterns reported in [7]. The beam shape is predicted with good accuracy although the measured patterns exhibit a certain asymmetric behaviour due to manufacturing tolerances and alignment errors. In addition, a more detailed simulation model of the 3D feeding section could potentially improve the accuracy. The addition of additional details in the 3D section would not influence the computation time during shaping of the lens because the admittance matrix of the feeding section is computed once and reused. The directivity of the leaky lens antenna is shown in Figure 5 for frequencies between 35 and 70 GHz. For comparison, the directivity was previously computed with CST in [2] and the measured gain of the antenna was reported in [7]. The directivity obtained with the generalised admittance matrix method agrees well with the CST results but the runtime is 1-2 minutes instead of hours.

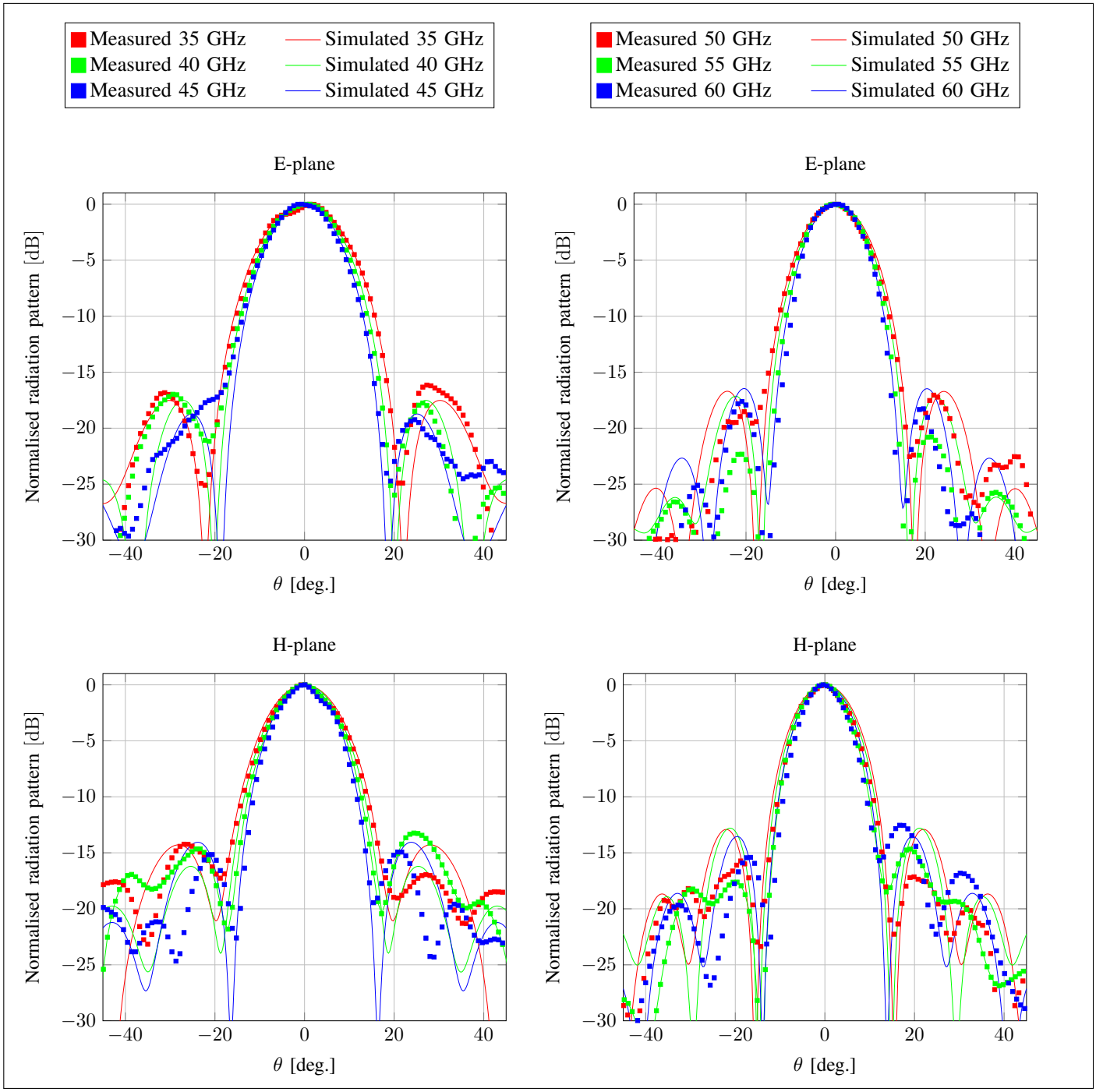

Fig. 4. Normalised radiation patterns of leaky lens antenna. Top row: Co-polar E-plane pattern. Bottom row: Co-polar H-plane pattern. Left column: 35 GHz, 40 GHz, and 45 GHz. Right column: 50 GHz, 55 GHz, and 60 GHz.

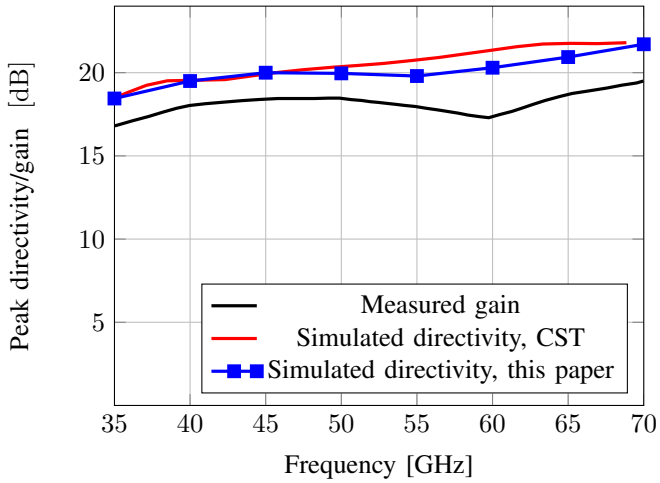

Fig. 5. Comparison of the measured gain of the prototype antenna reported in [7], the simulated directivity obtained by CST in [2], and the simulated directivity obtained by the method presented in this paper.

IV. Conclusion

We have presented a generalized admittance method that allows an antenna problem to be subdivided in multiple subdomains, with exact coupling between the domains. The method allows the admittance matrix to be computed with a higher-order 3D-MoM solver or a higher-order BoR-MoM solver. This combination is ideally suited for full-wave analysis of integrated lens antennas composed of a 3D feeding structure and an electrically large rotationally symmetric lens. The method has been applied to a planarly fed leaky lens antenna which have verified the excellent performance: At the highest operating frequency of the antenna, the full-wave solution can be obtained in two minutes. Furthermore, recomputation of the full solution is performed in one minute if the feeding section is unchanged. These computation times are orders of magnitudes faster than the methods applied in the past which allows full numerical optimisation of the lens performance without resorting to asymptotic methods.

References

[1] D. F. Filipovic, S. S. Gearhart, and G. M. Rebeiz, "Double-slot antennas on extended hemispherical and elliptical silicon dielectric lenses," *IEEE Trans. Microw. Theory Tech.*, vol. 41, no. 10, pp. 1738–1749, 1993.

[2] A. Neto, "UWB, non dispersive radiation from the planarly fed leaky lens antenna part 1: Theory and design," *IEEE Trans. Antennas Propagat.*, vol. 58, no. 7, pp. 2238–2247, Jul. 2010.

[3] A. V. Boriskin, G. Godi, R. Sauleau, and A. I. Nosich, "Small hemielliptic dielectric lens antenna analysis in 2-D: Boundary integral equations versus geometrical and physical optics," *IEEE Trans. Antennas Propagat.*, vol. 56, no. 2, pp. 485–492, Feb. 2008.

[4] E. Jørgensen, P. Meincke, and M. Sabbadini, "Fast and accurate design tool for rotationally symmetric reflector antennas with 3D waveguide components and support structures," in *Proc. 34th ESA Antenna Workshop*, Noordwijk, The Netherlands, 2012.

[5] E. Jørgensen and P. Meincke, "Domain-decomposition technique for efficient analysis of rotationally symmetric reflector systems containing 3D structures," *7th European Conference on Antennas and Propagation (EuCAP)*, pp. 1826 – 1830, 2013.

[6] E. Jørgensen, J. L. Volakis, P. Meincke, and O. Breinbjerg, "Higher order hierarchical Legendre basis functions for electromagnetic modeling," *IEEE Trans. Antennas Propagat.*, vol. 52, no. 11, pp. 2985–2995, Nov. 2004.

[7] A. Neto, S. Monni, and F. Nennie, "UWB, non dispersive radiation from the planarly fed leaky lens antenna part 2: Demonstrators and measurements," *IEEE Trans. Antennas Propagat.*, vol. 58, no. 7, pp. 2248–2258, Jul. 2010.